50: 543–551.
25. Stringham JC, Paulsen KL, Southard JH, et al. Prolonging myocardial preservation with a modified University of Wisconsin solution containing 2,3-butanedione monoxime and calcium. J Thorac Cardiovasc Surg 1994; 107: 764–775.
26. Jeschkeit S, Fischer JH. Effect of adding 2,3-butanedione monoxime to UW solution on poststorage functional recovery in blood-perfused rabbit hearts. Eur Surg Res 1998; 30(suppl 1): 53.
27. Rich TL, Langer GA. Calcium depletion in rabbit myocardium: calcium paradox protection by hypothermia and cation substitution. Circ Res 1982; 51: 131–141.
28. Fischer JH, Funcke C, Jeschkeit-Schubbert S, et al. Coronary endothelial function in heart grafts of non-heart-beating donors (NHBD) after 3 hr hypothermic cop-preservation and orthotopic transplantation. Eur Surg Res 2001; 33: 130–131.
29. Kuhn-Régnier F, Jeschkeit S, Bloch W, et al. Ultrastructural morphology of the endothelium and myocytes one week after heart transplantation and coronary oxygen persufflation in pigs. Thorac Cardiovasc Surg 2000; (suppl 1): 147.
30. Bosse M, Dahnken S, Fischer JH. Preserved endothelial function of large and small coronary vessels after prolonged storage including coronary oxygen persufflation. Eur Surg Res 2002; 34(suppl 1): 21 and Proceedings of the 37th Congress ESSR, Monduzzi Editore, Bologna 2002: 209–217.

0041-1337/03/7506-756/0
TRANSPLANTATION

Vol. 75, 756–761, No. 6, March 27, 2003
Printed in U.S.A.

NONINVASIVE IN VIVO ANALYSIS OF THE HUMAN HEPATIC MICROCIRCULATION USING ORTHOGONAL POLARIZATION SPECTRAL IMAGING

GERO PUHL,[1,4] KLAUS D. SCHASER,[2] BRIGITTE VOLLMAR,[3] MICHAEL D. MENGER,[3] AND UTZ SETTMACHER[1]

Background. **Analysis of hepatic microvascular perfusion in humans by direct imaging has been impossible so far. Orthogonal polarization spectral (OPS) imaging represents a new technology that combines simultaneous epi-illumination of the subject with linearly polarized light and noninvasive imaging of the microcirculation by reflectance spectrophotometry. The aim of this study was to evaluate the feasibility of studying the human hepatic microcirculation by OPS imaging in vivo and to define microcirculatory parameters for physiologic conditions.**

Methods. **The hepatic microcirculation was analyzed in four different regions of both liver lobes in 11 healthy individuals undergoing partial liver resection for living-donor liver transplantation. The optical probe was gently positioned on the liver surface and sequences of at least 20 sec per measurement were recorded by a charge-coupled device camera on videotape. Microhemodynamic parameters were quantified off-line by single-frame and frame-to-frame analysis using a computer-assisted image analysis system.**

Results. **OPS images of the hepatic microcirculation showed an acceptable quality with good resolution. Quantitative analysis revealed a sinusoidal red blood cell velocity of 0.97±0.43 mm/sec, a sinusoidal diameter of 8.8±0.9 μm, a sinusoidal volumetric blood flow of 58.2±9.6 pL/sec, an intersinusoidal distance of 22.6±2.5 μm, and a mean functional sinusoidal density of 391±30 cm^{-1}. Apart from the sinusoidal red blood cell velocity, all data of the parameters studied matched the pattern of normal distribution.**

Conclusions. **OPS imaging enabled for the first time direct in vivo visualization and quantification of the human hepatic microcirculation, providing significant insight into microvascular physiology of the human liver, to the extent that these data can be considered to represent physiologic values for human hepatic microcirculation.**

Experimental studies have elucidated hepatic microcirculatory dysfunction that occurs in response to ischemia and reperfusion, which is causative in the pathogenesis of organ failure. Major components of microvascular ischemia-reperfusion injury are leukocyte-endothelial cell interaction and endothelial disintegration, resulting in microcirculatory flow disturbances. These have been demonstrated in animal studies using in vivo fluorescence microscopy (*1–3*). This technique represents the only method allowing for both direct observation and quantification of the microcirculation within the individual segments of the hepatic microvasculature (*4*).

Experimentally, intravital fluorescence microscopy has been successfully used for microcirculatory analysis of different organs. However, the application of microvascular imaging techniques in humans is limited and has been impossible

[1] Klinik für Allgemein-, Viszeral- und Transplantationschirurgie, Charité Campus Virchow-Klinikum, Medizinische Fakultät der Humboldt-Universität zu Berlin, Berlin, Germany.
[2] Klinik für Unfall- und Wiederherstellungschirurgie, Charité Campus Virchow-Klinikum, Medizinische Fakultät der Humboldt-Universität zu Berlin, Berlin, Germany.
[3] Institut für Klinisch-Experimentelle Chirurgie, Universität des Saarlandes, Universitätsklinik Homburg/Saar, Homburg/Saar, Germany.
[4] Address correspondence to: Gero Puhl, M.D., Klinik für Allgemein-, Viszeral- und Transplantationschirurgie, Charité Campus Virchow-Klinikum, Medizinische Fakultät der Humboldt-Universität zu Berlin, Augustenburger Platz 1, 13353 Berlin. E-mail: gero.puhl@charite.de.

Received 25 September 2002. Revision requested 3 December 2002. Accepted 12 December 2002.

DOI: 10.1097/01.TP.0000056634.18191.1A

to use for the study of solid visceral organs. This is because of the large size of the intravital microscope setup and the requirement for use of fluorescent dyes, which are necessary for contrast enhancement and which themselves may be toxic and can produce phototoxic effects.

The new technology of orthogonal polarization spectral (OPS) imaging (*5*) has the potential to directly visualize and quantify microvascular perfusion of solid organs by advanced spectrophotometry. As was shown by Langer et al. (*6*), the OPS imaging technology can be used for the visualization of hepatic microcirculation during physiologic and pathophysiologic conditions in the rat liver. The results of this validation study showed a statistically significant agreement of the data obtained from OPS imaging and the standard method for such measurements, intravital fluorescence microscopy.

With the attempt to quantify human hepatic microvascular perfusion, numerous nonimaging techniques have been applied clinically, including thermodiffusion (*7*), laser Doppler flowmetry (*8*), polarographic oximetry, and inert gas clearance (*9*). In contrast to these indirect methods, the OPS imaging technology could represent a unique tool for intraoperatively assessing human hepatic microcirculation by direct measurement.

Studies to analyze human microcirculation using OPS imaging have been conducted on colonic-rectal mucosa (*10*), nailfold (*11*), brain (*10*, *12*), transcutaneously in term and preterm infants (*13*, *14*), cutaneously in the monitoring of wound healing (*15*), and sublingually in intensive care patients (*16*). Studies on solid visceral organs, such as the liver, have not been performed yet.

Because the hepatic microvasculature is regularly subjected to ischemia-reperfusion during liver surgery, intraoperative assessment of the hepatic microcirculation may provide new insights into human hepatic microvascular physiology. Therefore, the present study was designed to evaluate whether OPS imaging can be used for intraoperative imaging of sinusoidal perfusion and to quantitatively assess in vivo the physiologic hepatic microvascular parameters of healthy individuals undergoing partial liver resection for living-donor liver transplantation.

PATIENTS AND METHODS

The study protocol conformed to ethical guidelines of the 1975 Declaration of Helsinki as reflected by the approval of the local ethics committee. Informed consent in writing was obtained from all patients. Proof and safety of the OPS imaging system for clinical use are documented by the EC certificate of conformity No. GOD 00 10 41750 001 according to Annex IV, section 5 of council directive 93/42/EEC concerning medical devices, test report No. DM1V0113201 and DM 1V0113202 released with the above-mentioned certificate number by the certification body of TÜV Product Service (Munich, Germany).

OPS Imaging of the Liver Microcirculation

The entire system (Cytoscan; Cytometrics Inc., Philadelphia, PA) consists of an optical probe for homing the video microscope, and the base, which processes the images. The optical probe is connected to an external light source by means of a liquid light guide cable. With a standard video recorder (S-VHS, AG 7350-E; Panasonic, Matsushita Electric Ind., Osaka, Japan) and a standard video screen, online imaging and recording of the images can be performed. For illumination of the tissue, light is collected within the OPS imaging probe, passed through a spectral filter to isolate the wavelength of 548 nm (isobestic point of hemoglobin), and linearly polarized. The polarized light is than reflected toward the target by a beam splitter. An objective lens focuses the light onto a region approximately 1 mm in diameter. Light that is remitted from the target is collected by the same lens and passed through a second polarization analyzer orientated in a plane precisely orthogonal to that of the illumination, and the optical density of graduated gray scale is measured by transmission spectrophotometry to form an image of the illuminated region within the target on a charge-coupled device videocamera. Because polarization is preserved in reflection, photons scattered in the tissue contribute to the images, forming a virtual light source within the tissue by back-illumination. Hence, the contrast is obtained from absorption of the light by hemoglobin. Therefore, hemoglobin-carrying structures appear in a negative contrast, enabling the measurement of the vessel diameter, the length of the perfused vessels per observation area, the distance between the perfused vessels, and the red blood cell velocity within the vessel. The microcirculation can thereby be visualized using OPS imaging, similar to epi-illumination intravital microscopy (IVM) (*5*). The image is then transmitted to a video recorder for the off-line analysis. A final magnification of $\times$ 465 and a depth of focus of 200 to 500 μm is achieved on the video screen. For the intraoperative measurements, the probe, including the entire cable system, was packed into sterile foil (OpMi Drape; Zeiss Oberkochen, Germany).

Anesthesia

After premedication with 7.5 mg of midazolam administered orally, anesthesia was induced with thiopentone 4 to 6 mg/kg, fentanyl 0.1 mg, and vecuronium or *cis*-atracurium (0.1 mg/kg, respectively). Anesthesia was maintained with desflurane (4–6 vol%), nitrous oxide (50–70 vol%), and fentanyl as required. Intraoperative hemodynamic monitoring included continuous invasive arterial and central venous blood pressures. Hemodynamic management was directed to maintain normovolemia, avoiding central venous pressures above 5 mm Hg during the resection phase. All patients were extubated immediately after completion of surgery and transferred to the intensive care unit. For postoperative pain relief, patient-controlled analgesia was provided either intravenously or through an epidural catheter.

Experimental Protocol

Eleven donors (mean body weight, 64±9 kg; mean age, 44.2±15 years; male-to-female ratio, 3:8) undergoing partial liver resection for living-donor liver transplantation were examined. After laparotomy and before mobilization of the liver from the ligaments and preparation of the hepatic hilus structures, the baseline conditions of the microcirculation were recorded with the OPS imaging system. Therefore, the OPS probe was gently positioned on the upper and lower liver surfaces under physiologic saline immersion by hand, allowing stable video recordings. Using this technique, in vivo analysis of the hepatic microvasculature was performed in four regions on the surface of liver segments II and III and four regions on the surface of liver segments IV and VI in all patients. The microcirculation of each region of interest was recorded for 30 to 60 sec.

Microcirculatory Analysis

Quantification of the microhemodynamic parameters was performed off-line by single-frame and frame-to-frame analysis of the videotaped images using a computer-assisted image analysis system (CapImage; Zeintl, Heidelberg, Germany) (*17*). Analyses in the hepatic sinusoids were performed from eight areas of interest (acini) in each individual patient. The analyses of at least five sinusoids per acinus included the determination of sinusoidal diameter (D), intersinusoidal distance (ISD), and the red blood cell velocity (RBCV) within the sinusoids. The volumetric blood flow within the sinusoids (VBF) was calculated from the sinusoidal diameter and the red blood cell velocity: $VBF = \pi/4 \times D^2 \times RBCV$ (*18*), assuming cylindric geometry

of the sinusoids. Functional sinusoidal density (FSD), which is defined as the length of all blood cell perfused sinusoids per observation area (200×200 μm) and expressed in centimeters^{-1}, was assessed in accordance with the method described by Schmid-Schönbein et al. (*19*). Briefly, a grid system with a grid width representing 50 μm in vivo was superimposed on the video screen. By counting the intersections between the grid and the perfused sinusoids (N_s), FSD for each observation area was calculated: $FSD = \pi/2 \times N_s/L$, where L represents the total length of the grid system. The measurements resulted in 40 data points per individual patient for the D, ISD, RBCV, and VBF. The investigation of the FSD resulted in eight data points per patient.

Statistical Analysis

The results are expressed as mean±SD. The assumption of normality and homogeneity of variance was tested using the Kolmogorov-Smirnov test. Comparison of the within-subject variance and the between-subject variance did not show significant differences. Therefore, the observations of all patients were pooled for the frequency distribution and determined in histograms. To assess the degree of intraindividual inhomogeneities of the microcirculatory parameters, the index of heterogeneity was calculated for all parameters and patients by the coefficient of variance, that is, SD divided by the mean, as described previously in detail (*20*, *21*).

RESULTS

Macrohemodynamics

In all patients, macrohemodynamics were stable throughout the entire study period, with mean systolic and diastolic blood pressures of 119±7 and 64±8 mm Hg, a central venous pressure of 5.3±1.2 cm H_2O, a heart rate of 74±8 beats/min, an oxygen saturation of 98±1%, an $ETCO_2$ of 3.9±0.8 vol%, and a hemoglobin of 12.5±1.5 mg%.

General Characteristics

OPS imaging enabled well-contrasted and focused images of the human hepatic microcirculation. The video images obtained were of acceptable quality regarding the technical ability to image the red blood cells (RBC) without the need for fluorescence dyes. Hemoglobin-carrying cells appeared in a negative (black) contrast with the surrounding tissue. Direct imaging of cellular structures that lack hemoglobin, such as leukocytes or parenchymal and endothelial cells, could not be reliably performed. Accordingly, the vessel wall boundaries could not be visualized, and sinusoidal diameters were thus measured by the width of the intravascular RBC column. OPS imaging allowed the differentiation of portal venous branches, sinusoids, and postsinusoidal venules, and enabled the quantification of the microcirculatory parameters. The recordings of the microcirculation revealed homogeneous sinusoidal perfusion without indications for RBC sludging or sinusoidal perfusion stasis (Fig. 1).

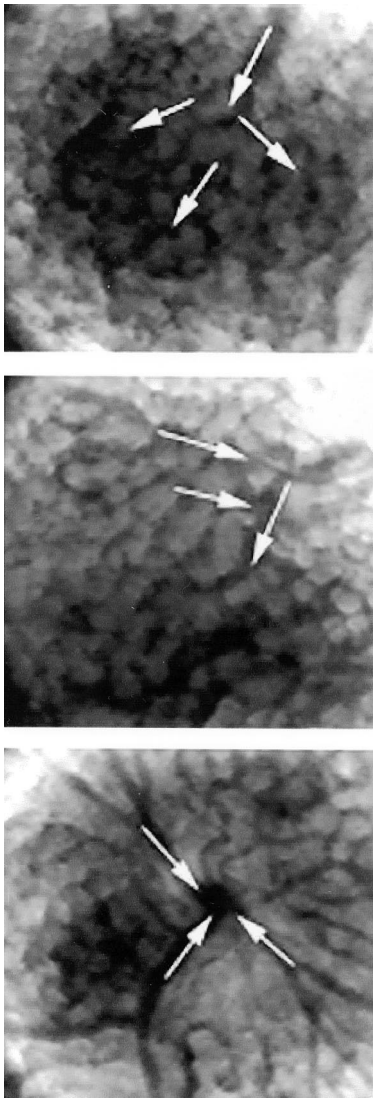

FIGURE 1. In vivo view of the human hepatic microcirculation by OPS imaging under physiologic conditions. The contrast is obtained by the absorption of light by hemoglobin-containing cells (i.e., erythrocytes). Therefore, the hemoglobin-carrying cells appear in a negative contrast compared with the surrounding tissue, and imaging of parenchymal and endothelial cells (e.g., the vessel wall) is not possible. The RBC are tightly packed as a column within the sinusoids, which represents the vascular lumen. (*A*) Acinar feeding vessel (*arrows*) delivering blood to the sinusoidal network. (*B*) Sinusoidal outflow tract (*arrows*) with sinusoids draining in a postsinusoidal venule. (*C*) Formation of a central venule branch (*arrows*) by postsinusoidal venules.

Sinusoidal Perfusion

Almost all sinusoids were found to be perfused with RBC, with a velocity ranging from 0.17 to 2.81 mm/sec and a mean of 0.97±0.43 mm/sec (Fig. 2). The heterogeneity index of 1.4±0.6 underlined the marked heterogeneity of sinusoidal RBC velocity, probably caused by the patient's respiration and the associated inferior caval vein pressure changes. The data of RBC velocity did not pass the normality test, which was expressed by a Kolmogorov-Smirnov distance of 0.0874 and a *P* value of 0.0098.

Sinusoidal diameters ranged from 6.8 to 11.6 μm, with a mean of 8.8±0.9 μm (Fig. 3). According to the sinusoidal RBC velocities and diameters, the volumetric blood flow within the individual sinusoids ranged from 19.2 to 140.5 pL/sec, with a mean of 58.2±9.6 pL/sec. Furthermore, the ISD ranged from 16.4 to 29.6 μm (mean, 22.6±2.5 μm) and the FSD ranged from 314 to 456 cm^{-1} (mean, 391±30 cm^{-1}) (Fig. 4). Data of sinusoidal D, ISD, FSD, and sinusoidal blood flow matched the pattern of normal distribution. An index of

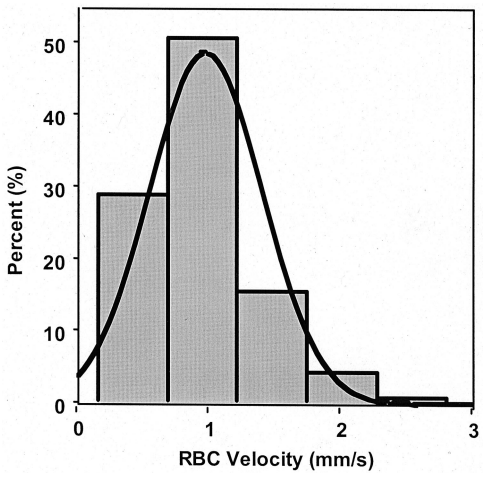

FIGURE 2. **RBCV in human hepatic sinusoids under physiologic conditions. Data are given in millimeters per second and are expressed as a frequency distribution with the mean at the top of the curve. RBCV data did not match the pattern of normal distribution (Kolmogorov-Smirnov test). A total of 440 single measurements were performed.**

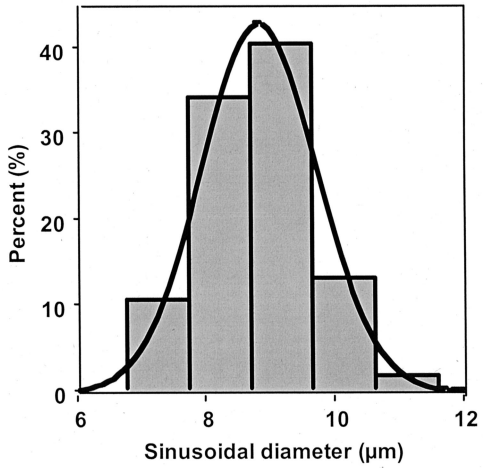

FIGURE 3. **Sinusoidal diameter of human hepatic sinusoids under physiologic conditions. Data are given in micrometers and are expressed as a frequency distribution with the mean at the top of the curve. The histogram expresses normal distribution of the total number of 440 single measurements (Kolmogorov-Smirnov test).**

heterogeneity of these parameters of less than 0.5 was considered to represent homogeneous distribution of perfusion.

DISCUSSION

The aim of this study was to evaluate the usefulness and feasibility of OPS imaging for the investigation of the human hepatic microcirculation. For the first time, the human liver microvascular architecture and perfusion could be directly visualized and quantitatively assessed in vivo in healthy individuals undergoing partial liver resection for living-donor liver transplantation. Therefore, these results may be considered to represent physiologic values of microvascular parameters of the human liver. On the basis of the high quality of the images and the possibility of quantitative analysis, the authors propose that OPS imaging is a useful and promising technique for providing further pathophysiologic information on the alterations of the human hepatic microcirculation in conditions that typically involve disorders of hepatic nutritional blood flow during surgery.

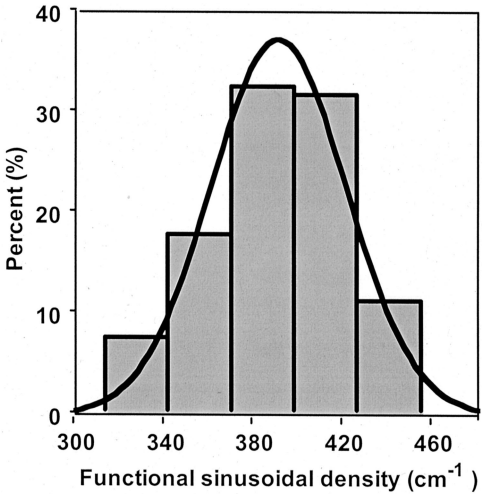

FIGURE 4. **FSD in the human liver under physiologic conditions. Data are given in centimeters^{-1} and are expressed as a frequency distribution with the mean at the top of the histogram. The histogram expresses normal distribution of the total number of 88 single measurements (Kolmogorov-Smirnov test).**

To date, the application of microvascular imaging techniques in humans is limited and has been impossible for the study of solid visceral organs. Existing experience includes capillaroscopy (*22*, *23*) and laser-scanning confocal imaging (*24*); however, these techniques restrict the visualization of the microcirculation in humans to easy accessible sites such as the nailfold, the conjunctiva, and the skin. Capillaroscopy therefore has been the only technique available for studying the human circulation at the microscopic level in vivo. Comparison between capillaroscopy and OPS imaging for imaging of human nailfold was made of the RBCV and capillary diameter, which showed similar results. Image quality of OPS imaging was superior to that of capillaroscopy (*11*).

Functional capillary density represents an established parameter for the quantification of nutritional tissue perfusion and an indirect measurement of oxygen delivery to the tissue (*25*). The algorithm for estimation of the functional capillary density in solid organs was originally described by Schmid-Schoenbein et al. for the exocrine pancreatic tissue (*19*, *26*). In the present study, functional sinusoidal density was defined as the length of the RBC-perfused sinusoids per observation area and is given in centimeters per centimeter^{-2}. Alternatively, the quality of the sinusoidal perfusion may be expressed by counting the number of perfused sinusoids crossing a horizontal raster line 200 μm long (*2*) and the determination of the sinusoidal perfusion rate, which expresses the percentage of the number of perfused sinusoids from all sinusoids visible (*27*). In the authors' opinion, determination of the FSD represents the preferable method for the OPS imaging technique, because non-RBC–perfused sinusoids are not visible, which makes the determination of the sinusoidal perfusion rate impossible.

The OPS imaging technology has been tested in standardized animal models of in vivo microscopy (*5*, *28*), including the rat liver (*6*, *29*). Comparison between OPS imaging and in vivo fluorescence microscopy revealed a statistically significant agreement of the results with respect to the image quality and the dimension of most of the microcirculatory parameters. Both methods image RBC adequately. A "functional sinusoid" is defined as a sinusoid that carries at least one RBC during a 30-sec observation period. At a physiologic hematocrit, the RBC column is tightly packed, with two distinct and smooth edges. Therefore, there is good agreement between IVM and OPS imaging to measure the FSD (*6*).

In addition to the FSD, in the present study the ISD was measured. This parameter is of particular importance, because an increase of ISD in response to pathologic insults such as ischemia-reperfusion may indicate edema formation caused by swelling of both endothelial and parenchymal cells. Alternatively, the ISD could also increase because of distinct sinusoidal no-flow with perfusion of just only every second or third sinusoid.

In contrast to IVM, OPS imaging does not allow the direct visualization and quantification of leukocytes, leukocyte-endothelial cell interactions, leukocyte activation, or platelets. Because OPS imaging visualizes RBC through the absorbance of hemoglobin in erythrocytes but not white blood cells, the leukocytes appear only indirectly, as the smooth boundary of the RBC column disappears and becomes pitted with gaps and holes caused by the edges of rolling and sticking leukocytes. However, these only occasionally visible events are insufficient in image quality and thus do not allow for quantitative analysis. Therefore, OPS imaging is currently limited for the measurement of parameters concerning the RBC column.

Furthermore, the differentiation of the various segments within the sinusoids (periportal, midzonal, pericentral), according to the zonal labeling resulting from the endothelial-hepatocellular transport of fluorescent compounds as reported by Gumucio et al. (*30*), which can be visualized by acridine orange on IVM, is not possible by OPS imaging. In contrast to IVM, however, OPS-imaging can be used to visualize the microcirculation in humans, because fluorescent dyes used for contrast enhancement, which may be directly toxic or produce phototoxic effects, are not required (*5*).

In the current study, analysis of the microhemodynamic parameters revealed some distinct differences compared with the well-established in vivo microscopic data of rat liver microcirculation. Specifically, the sinusoidal RBCV was found to be twofold higher compared with that observed in rat liver under physiologic conditions (*4*). Nonetheless, the remarkable heterogeneity of the human sinusoidal RBCV was similar to that in rat and mouse livers (*4*, *31*), which may indeed reflect the dependency of the liver microcirculation on changes of intrahepatic pressures resulting from respiration (*32*). Although the human and the rat liver sinusoidal diameters were comparable, the volumetric sinusoidal blood flow appears to be approximately 20% higher in human livers (*33*). In contrast, analysis of the FSD revealed an approximately 10% lower value in the human when compared with the rodent liver (*2*, *34*).

Even if OPS imaging is, like other microscopic techniques, restricted to the surface of the liver, it represents a unique and easy-to-handle technique for direct noninvasive measurement of the human hepatic microcirculation. Images obtained were of high quality and enabled off-line quantification of hepatic microhemodynamics, and which are now providing physiologic data on nutritive perfusion of the human liver. Furthermore, the technology allows for repeated measurements within the same window of investigation. It remains to be shown whether this technology will allow monitoring of the manifestation of ischemia-reperfusion–induced microcirculatory disorders intraoperatively. In addition, these future studies must demonstrate whether those microcirculatory disorders in ischemia-reperfusion correlate with the clinical course and outcome of the patients.

REFERENCES

1. Post S, Palma P, Rentsch M, et al. Hepatic reperfusion injury following cold ischemia in the rat: Potentials of quantitative analysis by in vivo microscopy. Prog Appl Microcirc 1993; 19: 152–166.
2. Clemens MG, McDonagh PF, Caudry ICH, et al. Hepatic microcirculatory failure after ischemia and reperfusion: Improvement with ATP-$MgCl_2$ treatment. Am J Physiol 1995; 248: H804–H811.
3. Vollmar B, Menger MD, Glasz J, et al. Impact of leukocyte-endothelial cell interaction in hepatic ischemia-reperfusion injury. Am J Physiol 1994; 267: G786–G793.
4. Menger MD, Marzi I, Messmer K. In vivo fluorescence microscopy for quantitative analysis of the hepatic microcirculation in hamsters and rats. Eur Surg Res 1991; 99: 158–169.
5. Groner W, Winkelman JW, Harris AG, et al. Orthogonal polarization spectral imaging: A new method for study of the microcirculation. Nat Med 1999; 5(10): 1209–1213.
6. Langer S, Harris AG, Biberthaler P, et al. Orthogonal polarization spectral imaging as a tool for the assessment of hepatic microcirculation. Transplantation 2001; 71: 1249–1256.
7. Klar E, Kraus T, Bredt M, et al. First clinical realization of continuous monitoring of liver microcirculation after transplantation by thermodiffusion. Transpl Int 1996; 9(1): S140–S143.
8. Arvidsson D, Svensson H, Haglund U. Laser Doppler flowmetry for estimating liver blood flow. Am J Physiol 1988; 254: G203–G209.
9. Mathie RT. Hepatic blood flow measurements with inert gas clearance. J Surg Res 1986; 41: 92–119.
10. Mathura KR, Ince C. First clinical use of orthogonal polarization spectral imaging. In: Messmer K, ed. Orthogonal polarization spectral imaging. Basel, Karger 2000, pp 94–101.
11. Mathura KR, Vollebregt KC, Boer K, et al. Comparison of OPS imaging and conventional capillary microscopy to study the human microcirculation. J Appl Physiol 2001; 91: 74–78.
12. Uhl E, Lehmberg J, Steiger H-J, et al. Intraoperative observation of human cerebral microcirculation. In: Messmer K, ed. Orthogonal polarization spectral imaging. Basel, Karger 2000, pp 72–81.
13. Christ F, Genzel-Boroviczény O, Schaudig S. Monitoring of the microcirculation in cardiac surgery and neonates using orthogonal polarization spectral imaging. In: Messmer K, ed. Orthogonal polarization spectral imaging. Basel, Karger 2000, pp 82–93.
14. Genzel-Boroviczény O, Strötgen J, Harris AG, et al. Orthogonal polarization spectral imaging (OPS): A novel method to measure the microcirculation in term and preterm infants transcutaneously. Pediatr Res 2002; 51: 386–391.
15. Klitzman B, Braun RD, Lockhart AC, et al. Wound-induced angiogenesis: A clinical model. In: Messmer K, ed. Orthogonal polarization spectral imaging. Basel, Karger 2000, pp 110–114.
16. De Baker D, Creteur J, Vincent J-L. Use of orthogonal polarization spectral imaging in intensive care. In: Messmer K, ed. Orthogonal polarization spectral imaging. Basel, Karger 2000, pp 104–109.
17. Zeintl H, Tompkins WR, Messmer K, et al. Static and dynamic video image analysis applied to clinical investigations. Prog Appl Microcirc 1986; 11: 1–10.
18. Gross JF, Aroesty J. Mathematical models of capillary flow: A critical review. Biorheology 1972; 9: 225–264.
19. Schmid-Schoenbein GW, Zweifach BW, Kovalcheck S. The application of stereological principles to morphometry of the microcirculation in different tissues. Microvasc Res 1977; 14: 303–317.

20. Tyml K, Budreau CH. Heterogeneity of microvascular response to ischemia in skeletal muscle. Int J Microcirc Clin Exp 1988; 7: 205–221.
21. Menger MD, Steiner D, Messmer K. Microvascular ischemia-reperfusion injury in striated muscle: Significance of "no reflow". Am J Physiol 1992; 263: H1892–H1900.
22. Wolf S, Arend O, Schulte K, et al. Quantification of retinal capillary density and flow velocity in patients with hypertension. Hypertension 1994; 23: 464–467.
23. Fenton BM, Zweifach BW, Worthen DM. Quantitative morphometry of conjunctival microcirculation in diabetes mellitus. Microvasc Res 1979; 18: 153–166.
24. Rajadhyaksha M, Grossmann M, Esterowitz D, et al. In vivo confocal scanning laser microscopy of human skin: Melanin provides strong contrast. J Invest Dermatol 1995; 104: 946–952.
25. Harris AG, Leiderer R, Peer F, et al. Skeletal muscle microvascular and tissue injury after varying durations of ischemia. Am J Physiol 1996; 271: H2388–H2398.
26. Vollmar B, Preissler G, Menger MD. Hemorrhagic hypotension induces arteriolar vasomotion and intermittent capillary perfusion in rat pancreas. Am J Physiol 1994; 267: H1936–H1940.
27. Lautt WW, Greenway CV, Legare DJ, et al. Localization of intrahepatic portal vascular resistance. Am J Physiol 1986; 251: G357–G381.
28. Harris AG, Sinitsina I, Messmer K. The Cytoscan model E-II, a new reflectance microscope for intravital microscopy: Comparison with the standard fluorescence method. J Vasc Res 2000; 37: 469–476.
29. Langer S, von Dobschuetz E, Harris AG, et al. Validation of the orthogonal polarization spectral imaging technique on solid organs. In: Messmer K, ed. Orthogonal polarization spectral imaging. Basel, Karger 2000, pp 32–46.
30. Gumucio JJ, Miller DL, Krauss MD, et al. Transport of fluorescent compounds into hepatocytes and the resultant zonal labeling of the hepatic acinus in the rat. Gastroenterology 1981; 80(4): 639–646.
31. MacPhee PJ, Schmidt EE, Groom AC. Intermittence of blood flow in liver sinusoids, studied by high resolution in vivo microscopy. Am J Physiol 1995; 269: G692–G698.
32. Neuhaus P, Blumhardt GAD. Extracorporeal liver perfusion: Applications of an improved model for experimental studies of the liver. Int J Artif Organs 1993; 16(10): 729–739.
33. Bauer M, Marzi I, Ziegenfuss T, et al. Comparative effect of crystalloid and small volume hypertonic hyperoncotic fluid resuscitation on hepatic microcirculation after hemorrhagic shock. Circ Shock 1993; 40: 187–193.
34. Ferguson D, McDonagh PF, Biewer J, et al. Spatial relationship between leukocyte accumulation and microvascular injury during reperfusion following hepatic ischemia. Int J Microcirc Clin Exp 1993; 12: 45–60.

0041-1337/03/7506-761/0
TRANSPLANTATION
Vol. 75, 761–769, No. 6, March 27, 2003
Printed in U.S.A.

THE METABOLIC AND MICROCIRCULATORY IMPACT OF ORTHOTOPIC LIVER TRANSPLANTATION ON THE OBESE ZUCKER RAT[1]

CHEUK-KWAN SUN,[2] XING-YI ZHANG,[2] ARTHUR ZIMMERMANN,[3] AND ANTONY M. WHEATLEY[2,4]

Background. **The purpose of this study was to investigate the metabolic alterations in the recipient and microcirculatory changes to the graft in the first 3 months after orthotopic liver transplantation (OLT) of nonsteatotic liver grafts from lean rats into obese Zucker rats.**

Methods. **Body weight and plasma lipids were measured for 3 months post-OLT. Graft perfusion (hepatic microcirculatory perfusion [HMP]) and vascular structure were measured in vivo at 3 months. Liver biopsy specimens were obtained throughout for morphologic analysis. Sham-operation obese and lean Zucker rats acted as controls.**

Results. **Plasma cholesterol levels were elevated from 2 months after OLT, whereas plasma triglyceride levels were reduced ($P<0.05$). Plasma high-density lipoprotein cholesterol concentrations increased from the first month after OLT ($P<0.05$). HMP in OLT animals (137±3 perfusion units [PU]) ($P<0.05$) was intermediate between lean (221±11 PU) and obese controls (113±5 PU). Hepatic cord width in the OLT group was similar to that in lean controls. Mean liver-to-body weight ratios in OLT animals (4.12%±0.39%) were significantly higher than in lean controls (3.25%±0.1%). The number of viable hepatocytes per high-power field in the OLT animals was lower than in the lean animals but higher than in obese controls ($P<0.05$). The transplanted livers showed moderate to marked microvesicular fatty change (MIFC) and glycogen deposition at 3 months after OLT.**

Conclusions. **Transplantation of a nonsteatotic liver into an obese Zucker rat initially has a positive effect on lipid metabolism. However, 3 months after OLT, the donor liver became steatotic with MIFC changes and reduced perfusion. The authors' results emphasize the importance of the recipient's metabolic status in the maintenance of liver graft function after OLT.**

Reports in the literature on the outcome of orthotopic liver transplantation (OLT) in obese and diabetic patients are few (*1*). Although much emphasis has been placed on the use of steatotic liver grafts in clinical liver transplantation, the suitability of OLT as a therapy in obese recipients has not

[1] Supported by the Royal Society of New Zealand Marsden Fund.
[2] Microcirculatory Research Laboratory, Department of Physiology, School of Medical Sciences, University of Otago, Dunedin, New Zealand.
[3] Department of Pathology, University of Berne, Berne, Switzerland.
[4] Address correspondence to: Antony M. Wheatley, Ph.D., Microcirculatory Research Laboratory, Department of Physiology, School of Medical Sciences, University of Otago, P.O. Box 913, Dunedin, New Zealand. E-mail: a.wheatley@otago.ac.nz.
Received 16 May 2002. Revision requested 17 July 2002. Accepted 13 November 2002.

DOI: 10.1097/01.TP.0000054680.70476.70